FINAL REPORT
February 25, 2019

Modified Natural Materials for Rendering Applications

Principal Investigator(s): Daniel C. Whitehead, Associate Professor
dwhiteh@clemson.edu
Department of Chemistry
467 Hunter Hall
Clemson University
Clemson, SC 29634
(864) 656-5765

Collaborators: Frank Alexis, Associate Professor
falexis@yachaytech.edu.ec

Date Submitted: February 24, 2017

Project Start Date: July 1, 2017

Duration of Project: 19 months

Lay Summary: This project continued our prolonged efforts toward the development of new functional materials for technologies to reduce odor emissions from the rendering industry. In the beginning of our work with FPRF, the main target of this work was to develop engineered, biodegradable poly(lactic acid) (*i.e.* PLA) nanomaterials whose surface could be decorated with appropriate reactive sites (*i.e.* functional groups) that would, in turn, capture or destroy malodorous volatile organic byproducts of rendering processes. Briefly, by decorating the nanomaterials with appropriate reactive sites, offending volatile byproducts were absorbed by the formation of either ionic or covalent bonds. In this manner, the malodorants were chemically modified so as to both harness them onto the biodegradable materials for disposal, and to render them less odorous. With previous FPRF funding, we successfully developed bench-scale technology that is capable of capturing targeted odorants associated with rendering processes. We have also parlayed FPRF support into further support from Clemson University Research Foundation in order to pursue scale-up and further optimization of our first generation materials and subsequent iterations. So far, this study has served as a proof-of concept exercise that unequivocally demonstrates that functionalized biodegradable poly(lactic acid) nanomaterials have the potential to become a next-generation strategy for odor remediation in the rendering industry. The materials work well for their intended purpose, and we have learned a lot about strategies toward engineering novel materials for odor capture. Along the way, our extensive exploration of our first generation polymeric materials based on the PLA platform have also uncovered some drawbacks that must be addressed on the way to a scalable product that can be applied at rendering facilities. The disadvantages of our first generation materials include: difficulty of synthesis, expense, batch-to-batch variation, difficulty scaling, and less than optimal thermal stability.

In an effort to address all of these issues, our 2016 ACREC/FPRF proposal sought to build upon our previous successes in order to parlay what we have learned during the investigation of our first generation materials into new strategies for the functionalization of cheaper, more-robust natural materials including cellulose and aluminosilicate clay substrates. As such, we successfully developed strategies for the modification of the much cheaper cellulose and clay platforms and have demonstrated that they are capable of capturing rendering malodorant VOCs. Importantly, these materials are easier to synthesize at a fraction of the cost. **This proposal** sought to expand upon these new, cheaper materials in order to 1.) further improve and vet their performance in malodorant VOC capture, 2.) evaluate their potential for rendering wastewater purification, and 3.) prepare related cellulose/clay platforms for the remediation of pesticide residue in rendered fats.

This long-term project has the potential to be very beneficial to the rendering industry. First, we are very close to realizing our goal of developing a scalable, cheap material for a next-generation alternative to established methods for odor remediation. In this context, the materials described herein might present several uses in an industrial setting. The materials could be employed as a rapid-use odor adsorbent in an emergency or spill situation. Further, the materials could, in principle, be incorporated into existing odor remediation equipment as an added means for odor elimination. The obvious long-term goal would be to develop an appropriate formulation of nanomaterials that would compete with or ideally supplant existing odor elimination measures. The potential also exists to apply our materials in other settings in the rendering industry in the context of wastewater purification. Aim 2 of this proposal sought to evaluate that potential.

Finally, our methods of preparation are modular, and thus may also be applicable to other uses including pesticide remediation from rendered fats, a strategy that was explored in the third aim of this proposal.

Objectives:

Aim 1: Capture of Malodorant VOC gases: To explore the nature of the poly(amine) functional group cap on the efficacy of gas capture and conduct follow-up on-site beta testing.

Aim 2: To evaluate poly(amine) clays and cellulose nanocrystals for rendering wastewater purification.

Aim 3: To prepare oxime modified clays and cellulose nanocrystals for the removal of pesticide contaminants from rendered fats.

Project Overview:

Aim 1: Capture of Malodorant VOC gases: To explore the nature of the poly(amine) functional group cap on the efficacy of gas capture and conduct follow-up on-site beta testing.

We divided this work into three Tasks.

In the first task, we sought to explore the nature of the amine cap on the efficacy of gas capture by modulating the amine region of our cellulose nanocrystals (CNCs). Briefly, we compared the performance of the poly(ethylenimine)-capped CNCs with two new formulations that used smaller, more economical caps: ethylenediamine (EN), and tris(2-aminoethyl)amine (TRIS). Thus, we successfully prepared EN-CNCs and TRIS-CNCs (Figure 1)by means of carbodiimide coupling using analogous conditions to our previously optimized protocol for the preparation of the first generation PEI-CNCs. The two CNC preparations bearing smaller amine caps were characterized by infrared spectroscopy and thermogravimetric analysis (Figure 1)

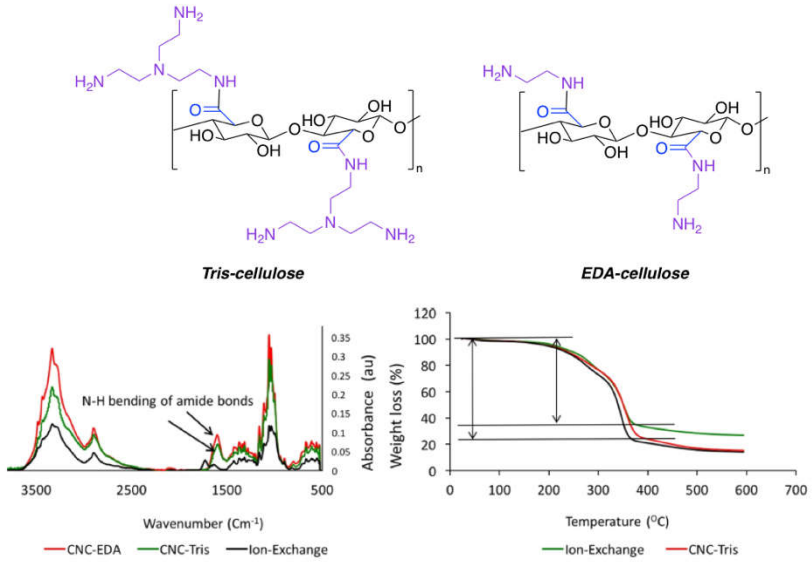

Figure 1. Successful preparation of Cellulose materials that explored the nature of the amine cap. Top: Chemical structures of cellulose modified with tris(2-aminoethyl)amine (i.e. Tris-CNC) and ethylenediamine (i.e. EDA-CNCs). Bottom left: Infrared spectroscopy characterization of new amine-capped CNCs. Bottom right: thermogravimetric analysis of new amine-capped CNCs.

After successfully developing a robust protocol for the synthesis of EDA-CNC and TRIS-CNC, we turned to an evaluation of their ability to capture target aldehyde VOCs (Figure 2). Thus, upon exposure of EDA-CNC and TRIS-CNC samples to hexanal vapors, the materials facilitated gas capture of 98.1% and 92.5% reduction, respectively. In the case of octanal, both EDA-CNC and TRIS-CNC materials facilitated 100% capture of the target VOC. Thus, this aim successfully demonstrated that the poly(amine) cap of our first generation cellulose materials can be successfully replaced with smaller, cheaper amine caps such as ethylenediamine or tris(2-aminoethyl)amine while still maintaining acceptable performance for gas capture.

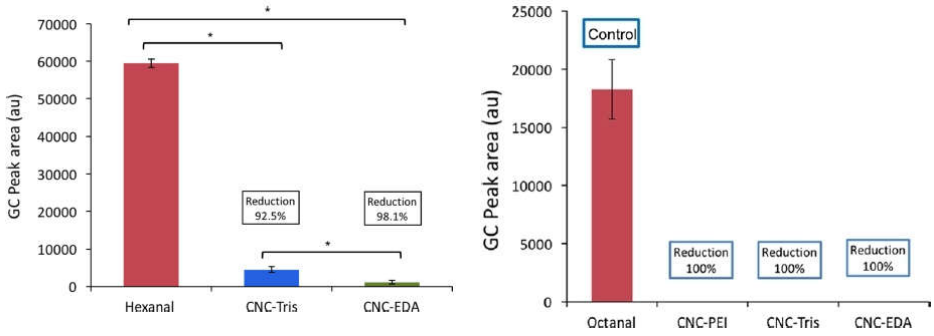

Figure 2. Evaluation of TRIS-CNC and EDA-CNC materials for capture of gaseous hexanal (left) and gaseous octanal (right). The data confirms that the amine-cap on the CNC materials can be modified to smaller, cheaper amines while maintaining acceptable performance for VOC capture.

In the second task, we investigated our poly(amine) capped kaolinite clay (i.e. Kao-PEI) material for the remediation of volatile carboxylic acids in ambient air at a rendering plant. Short-chain volatile fatty acids represent a major class of the detectable VOCs resulting from ambient air samples rendering facilities. In order to probe the usefulness of the Kao-PEI material for the remediation of volatile fatty acid VOCs associated with rendering operations, we designed a small-scale remediation experiment. Briefly, we generated packed cartridges containing 0.75 g of Kao-PEI packed between two cotton plugs and sealed in a glass tube. Prior to the in-plant sampling runs, the ends of the sealed tubes were opened with pliers and the Kao-PEI cartridges were plumbed in front of a commercially available KOH-coated silica gel cartridge designed for sampling Volatile Fatty Acids (VFA) using a short length of tubing. The other end of the VFA sample cartridge was plumbed to a sampling pump and plant air was collected at a rate of 700 mL/min over a 100 min sampling period. Thus, plant air was pumped first through the Kao-PEI sample cartridges prior to passing through the KOH-coated silica gel cartridge used to sample the VFA load of the sampling site. Sampling was conducted in this manner in triplicate using three sampling pumps in parallel. Triplicate untreated plant air samples were collected simultaneou

Table 1. Pilot-scale capture of volatile fatty acids from a rendering facility by Kao-PEI cartridges

Entry	Volatile Fatty Acids	Unreated (ppb)	Treated (ppb)	% Reduction
1	acetic acid	233.3 ± 5.8	< 8	> 97%
2	propanoic acid	163.3 ± 5.8	1.9 ± 1.1	99%
3	2-methylpropanoic acid	17.0 ± 1.0	0.9 ± 0.4	95%
4	butanoic acid	180.0 ± 10.0	2.0 ± 1.7	99%
5	2-methylbutanoic acid	11.7 ± 0.6	< 0.6	> 95%
6	3-methylbutanoic acid	11.3 ± 0.6	< 0.6	> 95%
7	pentanoic acid	19.7 ± 1.2	< 0.6	> 97%
8	4-methylpentanoic acid	6.9 ± 0.5	< 0.5	> 93%
9	hexanoic acid	10.0 ± 0.9	< 0.5	> 95%
10	heptanoic acid	1.6 ± 0.2	< 0.5	> 69%
11	octanoic acid	1.7 ± 0.2	< 0.5	> 71%
12	nonanoic acid	1.0 ± 0.1	< 0.4	> 60%

sly. This sampling regime was then repeated on the next day. After the VFA sampling cartridges were treated with plant air for 100 min, they were sealed and sent to a commercial atmospheric analysis laboratory for volatile fatty acid analysis using a standardized GC/MS protocol.
The results of this in-plant analysis show that the Kao-PEI material significantly reduces the VOC load of all detectable volatile fatty acids in comparison to the untreated plant air samples (Table 1). Untreated plant air samples revealed part-per-billion level concentrations of twelve fatty acids ranging from 233 ± 5.8 ppb for acetic acid to 1 ± 0.1 ppm for the less-volatile nonanoic acid. In comparison, the treated plant air, having passed first through the Kao-PEI cartridge prior to passing through the VFA sample cartridge, returned analyses below the limit of detection for all volatile fatty acids except for propanoic acid (1.9 ± 1.1 ppb), 2-methylpropanoic acid (0.9 ± 0.4), and butanoic acid (2.0 ± 1.7). Nonetheless, in the case of these three analytes, Kao-PEI treatment of the plant air reduced these constituents by 99, 95, and 99%, respectively. Ultimately, this study represents an important step in demonstrating the applicability of PEI-modified kaolinite clay and other functionalized naturally occurring clays in VOC mitigation in an industrial setting.

In the third task, we explored the use of a new platform based on porous and nonporous microparticles arising from PLA-PEG-COOH and PLGA polymers. The ultimate goal of this portion of the present study was to investigate a strategy for the tunable formulation of porous and nonporous microparticles (MPs) of poly(D,L-lactic acid)-poly(ethylene glycol)-COOH (PDLLA-PEG-COOH) or poly(D,L-lactide-co-glycolide) (PLGA) copolymers, and to evaluate their performance in the capture of aldehyde VOCs. Thus, we arrived at a tunable process resulting in the preparation of porous and nonporous PDLLA-PEG-COOH MPs (1-2 μm diameter) as well as porous and nonporous PLGA MPs (100 μm and 50 μm, respectively). Thereafter, all four MP formulations were coated with PEI by means of an ultrasonication technique. The results of this strategy and the VOC capture performance of the various new materials are described below

Preparation of naked and PEI-coated porous and nonporous MPs

Two kinds of amphiphilic biodegradable polymers, namely PDLLA-PEG-COOH and PLGA, were employed to prepare MPs of different sizes, porous/smooth surface morphologies, and PEI surface coatings for their evaluation for the remediation of aldehyde VOCs. To formulate the MPs for this study, a commercially available PLGA (65/35) copolymer (*i.e.* 65% lactide and 35% glycolide) and a PDLLA-PEG-COOH copolymer were employed. The latter was synthesized via a ring opening polymerization method (*i.e.* the reaction of (D,L)-lactide and hydroxyl polyethylene glycol carboxyl in the presence of catalytic tin(II) 2-ethylhexanoate. The synthesized PDLLA-PEG-COOH polymer structure was then elucidated by ^{1}H NMR revealing three characteristic signals at 5.04, 3.64 and 1.68 ppm, corresponding to (C<u>H</u>-CH_3), (C<u>H_2</u>-C<u>H_2</u>)-O, and (CH-C<u>H_3</u>) respectively (See supporting information for spectrum). Next, MPs of the two polymers were fabricated following a slightly modified emulsion/solvent evaporation protocol in the presence of the stabilizer/surfactant (PVA). During the formulation process, we found that the size and morphology of the MPs could be modulated in a controlled manner by tuning some parameters such as *(i)* the inner aqueous phases, *(ii)* volume and nature of the organic solvent, *(iii)* solvent removal rate, *(iv)* concentration of the polymers and stabilizing agent (PVA), *(v)* concentration of the ammonium bicarbonate (NH_4HCO_3) foaming agent, and *(vi)* the drying

technique (*i.e.* either spray drying or freeze drying). By leveraging the systematic tuning of these parameters, we eventually arrived at protocols that reliably and reproducibly provided access to nonporous or porous PDLLA-PEG-COOH MPs exhibiting an average diameter of approximately 1-2 µm and nonporous or porous PLGA MPs of 50 and 100 µm diameter, respectively. The nonporosity or porosity of the various MP formulations was evaluated by scanning electron microscopy (SEM).

Scanning electron microscopy

The size, shape and surface morphology of the MP formulations was probed by SEM. Briefly, after preparation and drying of the MPs ,1-2 mg of each sample was deposited on a carbon grid without coating agent and imaged by SEM. Figure 3A depicts several views of the nonporous PDLLA-PEG-COOH MPs, illustrating the isolation of 1-2 µm MPs exhibiting a rather smooth surface morphology. By changing the formulation protocol and adding NH_4HCO_3 as a foaming agent during the preparation, MPs of similar diameter were isolated that clearly exhibited uniform porosity on the surface of the material (Figure 3B). Similarly, PLGA MPs were produced in both nonporous (50 µm diameter) and porous (100 µm) variants.

We assume that the controlled generation of porosity on the MP surfaces might arise for the confluence of several factors. The solvent evaporation rate in the oil phase might contribute to the formation of porosity. Shi *et al.* found that the removal rate of solvent can have a large effect on the porosity of the resultant material.[20] Finally, the inclusion of ammonium bicarbonate as a foaming agent likely plays a dual role in the formulation: first to stabilize the emulsion and prevent the aqueous droplets from aggregation during the removal of organic solvent, and second to generate pores by means of the rapid liberation of CO_2.

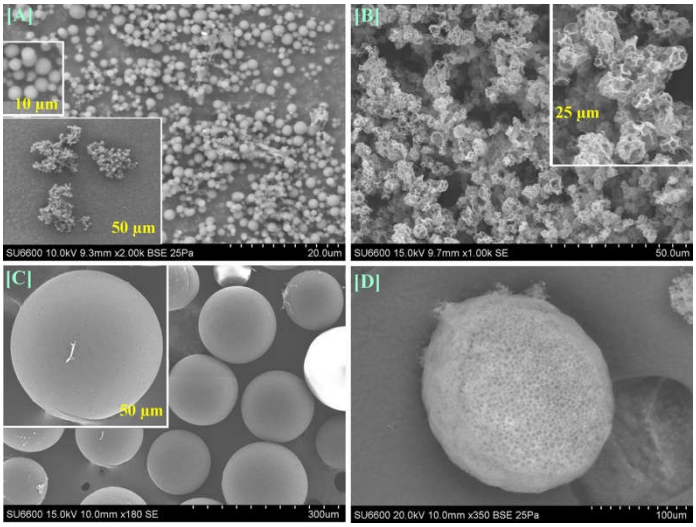

Figure 3. SEM images of different kinds of formulated microparticles. [A] Nonporous PDLLA-PEG-COOH MPs, [B] porous PDLLA–PEG-COOH MPs, [C] nonporous PLGA MPs, and [D] porous PLGA MPs.

Infrared spectra analysis

Figure 4 shows the Fourier transform infrared (FT-IR) spectra of both PDLLA-PEG-COOH and PLGA polymeric MPs demonstrating that the formulation process does not appreciably alter the chemical composition of the base polymeric materials. An IR spectrum the PVA stabilizing agent is included as well, and illustrates that this material is not incorporated into the resulting MPs to a significant extent despite its presence in the formulation protocol. The key, characteristic infrared signatures were observed for the PDLLA-PEG-COOH copolymer

structure both before and after nonporous MP formulation (Figure 4A): a low absorbance, broad peak at 3517 cm^{-1} (OH stretching due to the polymer termini or adventitious water), peaks at 2998, 2948, and 2885 cm^{-1} attributed to sp^3 C-H stretching, 1745 cm^{-1} arising from carbonyl stretching, and 1079 cm^{-1} arising from C-O stretching. The IR of porous MPs were indistinguishable from the spectra depicted in Figure 2A.

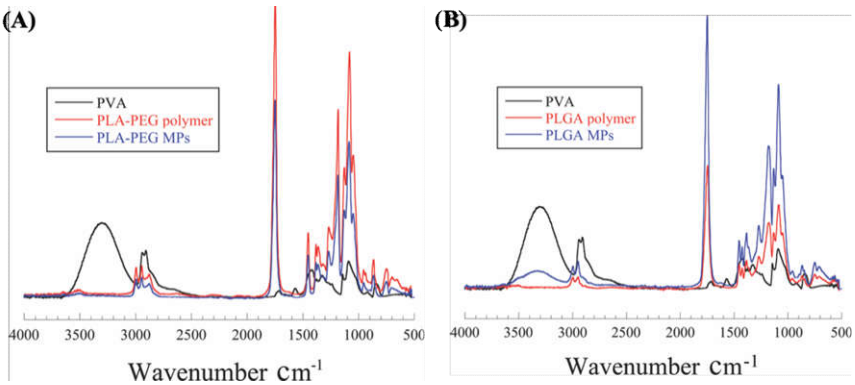

Figure 4. Representative FT-IR spectra of smooth PDLLA-PEG-COOH MPs (A) and porous PLGA MPs (B) and their parent polymers used in formulation (PVA, PDLLA-PEG-COOH, and PLGA pure polymers). The IR spectra of porous PDLLA-PEG-COOH MPs were indistinguishable from the spectra of the nonporous MPs depicted in A. The IR spectra of nonporous PLGA MPs were indistinguishable from the spectra of the porous MPs depicted in B.

Similarly, Figure 4B shows the overlaid spectra for the PVA stabilizer, PLGA polymer and PLGA porous MPs after preparation. Again, the pre- and post-formulation PLGA materials are virtually identical and the MPs show no evidence of PVA despite its presence as a stabilizer in the protocol. Briefly, the key features of the IR spectrum of the PLGA copolymer/MP formulation are: 3494-3580 cm^{-1} (O-H stretching from polymer termini or adventitious water), 3020, 2927 cm^{-1} (sp^3 C-H stretching), 1749 cm^{-1} (C=O stretching), and 1083, 1172 cm^{-1} (C-O stretching). The IR trace for nonporous PLGA MPs is indistinguishable from the spectra depicted in Figure 4B.

Overall, the FT-IR data demonstrated that both PDLLA-PEG-COOH and PLGA microparticles exhibit nearly identical IR signatures to their parent polymers prior to formulation. This result clearly demonstrates that the chemical composition of the polymers is unchanged during the course of the MP preparation.

TGA analysis

TGA analysis also confirmed very little change to the chemical composition of the materials after MP formulations, and further confirmed that the PVA stabilizer employed in the formulation step is not incorporated into the MPs. TGA curves for PVA, PDLLA-PEG-COOH polymer and nonporous PDLLA-PEG-COOH MPs appear in Figure 5A which indicates that there were slight mass losses in the range of 25 to 100 ˚C for all samples attributed to the loss of adsorbed water, although the PDLLA-PEG-COOH polymer sample (*i.e.* prior to MP formulation) contained significantly more water than both PVA and the PDLLA-PEG-COOH MPs. The PVA degradation curve shows a three-stage decomposition profile, where the first stage accounted for about 37% weight loss occurring between 107 and 201 ˚C, followed by 46% weight loss between 261 and 326 ˚C, and 9% weight loss between 386 and 505 ˚C. The PDLLA-PEG-COOH polymer exhibited a three-stage degradation process, where the first stage accounted for 7% weight loss between 108 and 204 ˚C (presumably due to the release of

significant amounts of adsorbed water), followed by a significant weight loss of 77% between 230 and 304 ˚C which likely corresponds to the thermal decomposition of the PDLLA-PEG-COOH polymer itself. The third stage was a 9% mass loss occurring over the range of 378 to 439 ˚C. Importantly, the nonporous MPs (evidently anhydrous after their prolonged drying following formulation) revealed a two-stage degradation profile, where the first stage accounted for an 87% mass loss occurring between 220 and 310 ˚C, which is similar to the major mass loss observed for the PDLLA-PEG-COOH parent material prior to MP formulation. These data provide further evidence that the chemical composition of the PDLLA-PEG-COOH polymer is unchanged during course of the MP formulation process. TGA traces for porous PDLLA-PEG-COOH MPs were indistinguishable from the TGA trace of the nonporous congener depicted in Figure 5A.

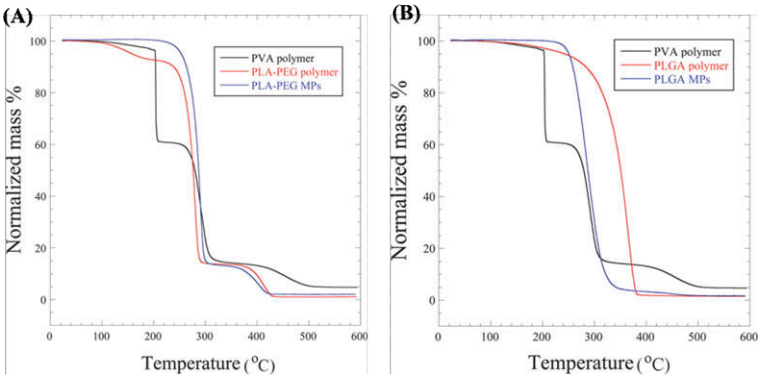

Figure 5. A: TGA analyses of PVA, PDLLA-PEG-COOH polymer and nonporous PDLLA-PEG-COOH MPs, and B: PVA, PLGA polymer and porous PLGA MPs. Note: TGA traces for porous PDLLA-PEG-COOH MPs were indistinguishable from the nonporous MP sample depicted in A and TGA traces of nonporous PLGA MPs were indistinguishable from the porous MP sample depicted in B.

Likewise, Figure 5B clearly distinguishes the single-stage degradation process observed for the PLGA polymer and the resulting nonporous MPs as compared to the three-stage degradation of the PVA stabilizing agent. Again, the TGA trace of the porous PLGA MPs is virtually identical to the trace for the nonporous MPs depicted in Figure 5B. These results further underscore that the PVA stabilizer is not incorporated into the MPs during the formulation process.

Almost 100% mass loss was observed during a rather gradual, one-stage degradation of the parent PLGA polymer over the temperature range from 110 to 400 ˚C. Interestingly, the PLGA MPs exhibited a much sharper one-stage degradation profile corresponding to a 97% mass loss that initiated at 220 ˚C and ended at 360 ˚C. While it is not immediately clear what contributed to the sharper degradation profile of the PLGA MP samples as compared to their parent polymer, the one-stage degradation profile for both materials over roughly the same temperature window suggests that the polymer formulation is likely unchanged over the course of the MP formulation.

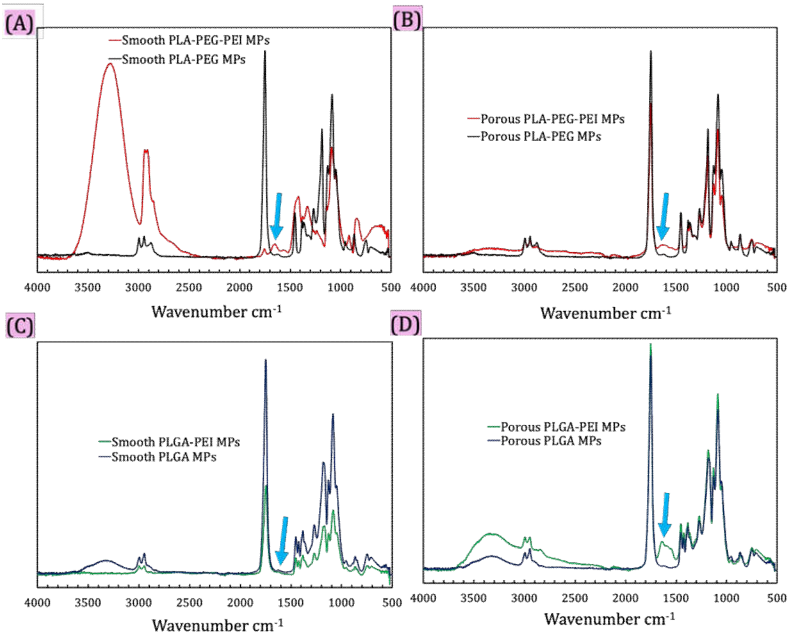

Figure 6. FT-IR data of the eight microparticles; nonporous and porous PDLLA-PEG-COOH MPs and their PEI functionalization (A and B), respectively. Nonporous and porous PLGA MPs and their PEI functionalization (C and D), respectively.

PEI coating of porous/nonporous MPs

Next, we sought to coat the porous/nonporous MP formulations described above with polyethylenimine (PEI) polymer. Our previous studies have demonstrated that materials surface-coated with PEI exhibit excellent VOC capture performance.

The MPs were coated with PEI by means of a one-pot ultrasonication protocol over 10 min followed by additional stirring for 6 h to allow for complete coating, presumably mediated by electrostatic interactions between the cationic PEI coat with the anionic carboxylates decorating the surface of the porous and non-porous MPs.

Figure 6 indicates changes to the FT-IR spectra of the porous and nonporous MP materials after PEI coating. Bands emerging in the region around 1600 cm^{-1} (indicated by blue arrow), attributable to N-H bending, provided the clearest evidence for the successful PEI coating event. The peak intensities in this region appear to be higher for the PEI-coated porous MPs than their nonporous congeners, which appear to have incorporated relatively little PEI. Indeed, in the case of the nonporous PLGA MPs (Figure 6C), there is little evidence for the successful incorporation of PEI based on the IR results. The more successful coating of the porous MPs can be attributed higher surface area of the porous materials as compared to their smooth, nonporous counterparts. The PEI-coated MPs were also characterized by TGA analysis (data not shown).

SEM-EDX Analysis of PEI-Coated MPs

The size, shape and surface morphology of the MP formulations was probed by scanning electron microscopy coupled with energy dispersive X-ray spectroscopy (SEM-EDX).

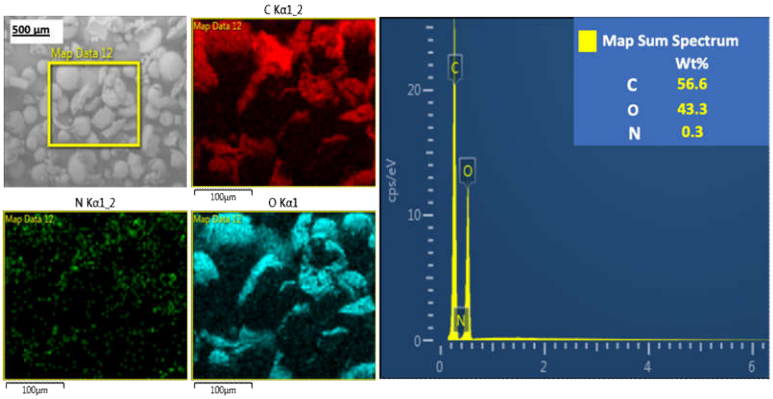

Figure 7. SEM-EDX analysis of the nonporous PLGA MPs after attempted PEI coating, indicating rather poor PEI coating.

We were also able to probe the extent to which PEI was coated on the surface of the MPs by means of SEM-EDX analysis. Using this technique, the relative success of the PEI-coating step was judged by quantifying the percentage of nitrogen present on the surface of the PEI-coated MPs.

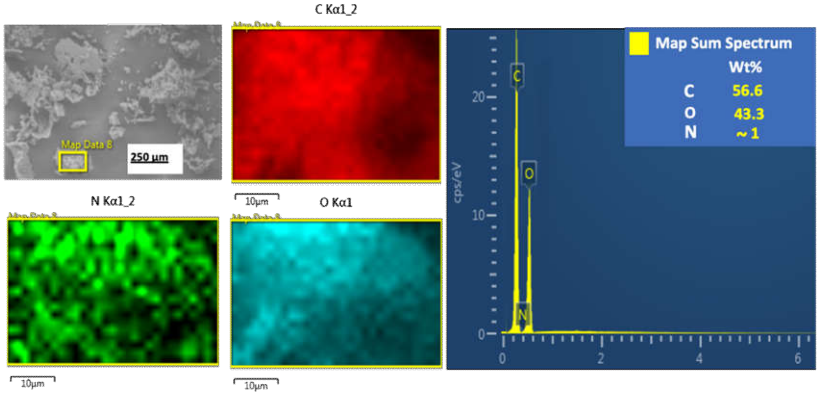

Figure 8. SEM-EDX analysis of PEI-coated porous PDLLA-PEG-COH MPs indicating a comparatively more efficient surface coating.

Thus, we chose two PEI-MP formulations for comparison by SEM-EDX analysis. For this study, we used the results depicted in Figure 6 to select a formulation that indicated a relatively high level of PEI incorporation, (*i.e.* PEI-coated porous PDLLA-PEI-COOH MPs, see Figure 6B) and a formulation that indicated almost no PEI incorporation (*i.e.* PEI-coated nonporous PLGA MPs, see Figure 6C) as judged by the relative intensity of the N-H bending signals around 1600 cm^{-1}. The SEM-EDX results of this comparison are depicted in Figures 7 and 8 and clearly indicate a corollary between enhanced N-H bending signals in the IR and nitrogen percentage on the surface of the MP. Thus, the nonporous PLGA material indicated just 0.3% nitrogen on the surface of the MP with rather sparse dispersion (see green channel in Figure 7). In sharp contrast, the PEI-coating of the porous PDLLA-PEG-COOH MPs evidently proceeded with higher efficiency, where SEM-EDX analysis revealed 1% N presence on the surface of the MP with rather uniform dispersion (see green channel in Figure 8). We hypothesize that the rough surface morphology and greater surface area of the porous materials allows for a more efficient and more steadfast PEI coating. Finally, we also observed that there is no change in the gross surface morphology or overall size of the MPs after PEI treatment as compared to the uncoated counterparts.

Gas chromatography assays

After developing a tunable and reliable protocol for the formulation of both PEI-coated and naked porous and nonporous microparticles, we next pivoted to the evaluation of these new materials for their ability to capture two prototypical VOCs of the aldehyde functional group class. To accomplish this task, we followed the standard gas capture protocol that we have previously described elsewhere. A 10 mg sample of each of the eight MP formulations outlined above were evaluated by incubating the material in the presence of hexanal and octanal vapors at 25 ˚C for 30 min, after which the headspace of the GC vial was analyzed. In parallel, we incubated untreated hexanal and octanal vapors at 25 ˚C for 30 min in the absence of MPs to serve as controls upon headspace analysis. Trial runs and control experiments were conducted in a series of five replicates. The headspace of the untreated samples was also analyzed as a control. The results of this study are depicted in Figures 9 and 10 for hexanal and octanal, respectively. Interestingly, all of the MP formulations successfully reduced the amount of VOC vapors in the

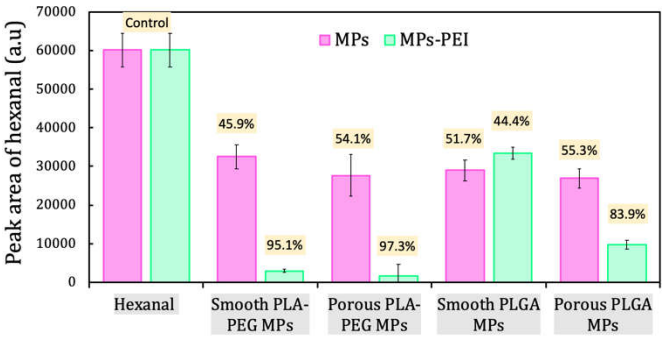

Figure 9. Gas chromatography assays for each of the developed microparticles against hexanal gas Results are presented as means ± standard deviation and all runs were repeated five times.

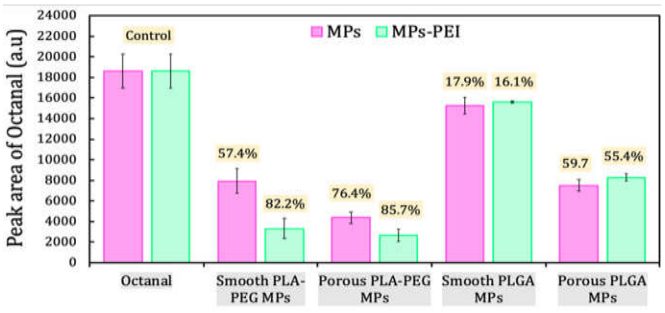

Figure 10. GC measurements for the same microparticles against octanal vapors. Results are presented as means ± standard deviation and all runs were repeated five times.

headspace as compared to untreated control samples. Figure 9 illustrates the GC assay of the four naked MPs and their PEI caps for the removal of hexanal gas. Thus for the naked PDLLA-PEG-COOH MPs, hexanal vapors were reduced by roughly 50% and 54% for the nonporous and porous MPs, respectively. In contrast, after surface-coating with PEI, these materials reduced the hexanal vapors in the headspace by approximately 95% and 97% for the nonporous and porous MPs, respectively.

For the naked PLGA MPs, both the nonporous and porous formulations facilitated about 52% and 55% removal of hexanal vapors. Unlike the coated PEG-PEI-COOH MPs described above, attempted PEI-coating of the PLGA materials provided mixed results. From both the IR and SEM-EDX analyses it was clear that the PEI-coating was poorly effective on the nonporous PLGA material. Consistent with these observations, the nonporous PLGA MPs isolated after the PEI coating experiment afforded no improvement on their initial VOC capture performance. In fact, the attempted PEI coating of that material returned MPs that performed slightly worse in the capture of hexanal vapors (*cf.* 44% capture versus 52% prior to coating). Evidently, the smooth morphology of the rather large (*i.e.* ~50 μm diameter), nonporous PLGA MPs is not conducive for effective PEI coating.

In comparison, the PEI-functionalized porous PLGA MPs showed a significantly higher capture efficiency of ~84% as compared to the naked, porous congeners that facilitated ~55% capture.

Moreover, all eight of the MP formulations were also evaluated for the capture of the less-volatile octanal. The naked PDLLA-PEG-COOH MPs exhibited a similar behavior with octanal (Figure 10) to that observed with hexanal. Specifically, the capture efficiency of the naked, porous PDLLA-PEG-COOH MPs was higher than the naked, nonporous congener (*i.e.* 76% removal versus 57% removal, respectively). The PEI-coated materials both demonstrated a further increase in the capture of octanal vapors, affording 82% and 86% removal for the PEI-coated nonporous and porous PDLLA-PEG-COOH materials, respectively.

In the case of octanal vapor remediation with the PLGA MP formulations, the naked, porous MPs significantly outperformed the nonporous congeners (*cf.* approximately 60% removal versus just 18% removal). Further, the PEI-coating event offered no improvement on the capture efficiency of these materials as compared to the non-coated porous and nonporous PLGA MP congeners.

The results of this task of Aim 1 describe the effective development of a new class of polymeric microparticles that can be tuned to display a smooth or porous surface morphology. The materials sometimes possess the intrinsic ability to capture VOCs. These materials can then be coated with PEI, which in turn can enhance the gas capture ability of the materials. This study represents the development of a new class of functional materials for VOC capture.

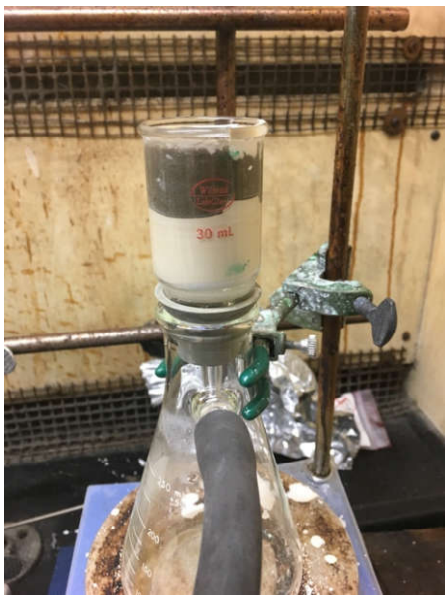

Figure 11. Experimental set-up for evaluation of clay materials for wastewater purification.

Aim 2: To evaluate poly(amine) clays and cellulose nanocrystals for rendering wastewater purification.

We first attempted to evaluate the performance of the poly(ethylenimine) kaolinite (Kao-PEI) clay materials for wastewater purification. A member company provided wastewater samples and grease-trap samples for experimentation. We developed a simple lab-scale experiment to filter the wastewater samples with Kao-PEI (Figure 11).

We used this set-up to evaluate the potential for the use of Kao-PEI to filter wastewater. During this investigation, we encountered a significant roadblock. We discovered that the poly(amine) cap on the kaolinite clay is not stable to prolonged exposure to water. Recall that the poly(amine) is installed onto the surface of the clay materials by non-covalent, electrostatic interactions. Thus, upon exposure of the Kao-PEI samples to water or methanol, we noted the rapid removal of the poly(amine) cap. The clay samples that we isolated after the wash step were indistinguishable from non-functionalized clay samples by means of thermogravimetric analysis. (Figure 12).

This disappointing result clearly indicated to us that the PEI-Kao material would not be suitable as a platform for treating rendering waste water. With this in mind, we decided that our PEI-functionalized cellulose materials (PEI-CNCs) might be more amenable as a platform for wastewater remediation because the PEI functionality is covalently attached to the cellulose substrate, and thus not susceptible to hydrolysis. We are still planning to evaluate the PEI-CNCs for this application, but we were unable to do so in this funding period because at the time, we had not yet optmized the synthesis of the CNC-PEI materials at a sufficiently large scale.

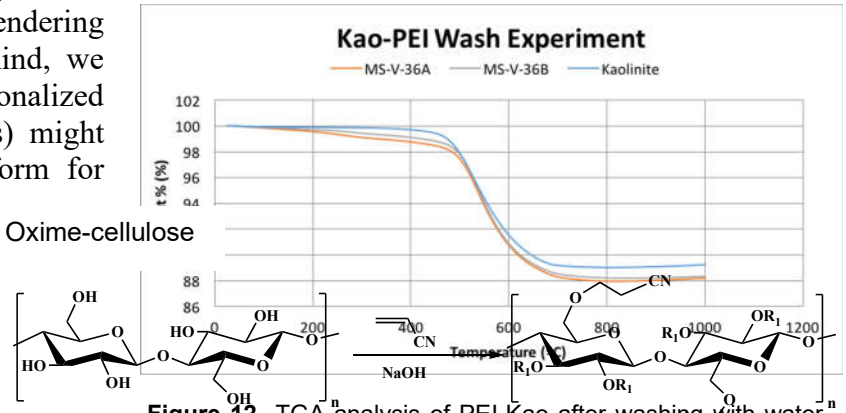

Figure 12 TGA analysis of PEI-Kao after washing with water (orange trace) and methanol (grey trace). The samples were indistinguishable from unmodified kaolinite (blue trace).

Aim 3: To prepare oxime modified clays and cellulose nanocrystals for the removal of pesticide contaminants from rendered fats.

Oxime-cellulose

Poly(oxime)-acrylonitrile polymer

; R1= H or CH_2CH_2CN
R2= H or $CH_2CH_2C(NH_2)$=NOH

Figure 13. Synthetic scheme for the preparation of oxime-cellulose materials and poly(oxime) acrylonitrile polymers.

In this aim, we set out to explore whether we could engineer functional materials that were capable of removing pesticide contaminants from rendered fats. To explore this goal, we first set out to modify cellulose or other polymeric materials to displace oxime functional groups on their surface. Oxime functional groups have been demonstrated previously to capture organophosphorus pesticides. Thus, we successfully prepared three formulations: Oxime-grafted cellulose nanocrystals, oxime-grafted cellulose microcrystals, and a poly(oxime) acrylonitrile polymer. The cellulose materials were prepared by conjugate addition of acrylonitrile onto the C6 carbinol of cellulose followed by trapping of the nitrile with aqueous ammonium hydroxide (Figure 13, top). Similarly, the poly(oxime) acrylonitrile material was prepared by treatment of polyacrylonitrile with ammonium hydroxide (Figure 13, bottom). These materials were characterized by a combination of infrared spectroscopy and thermogravimetric analysis (Figure 14 for oxime-cellulose and Figure 15 for poly(oxime) acrylonitrile).

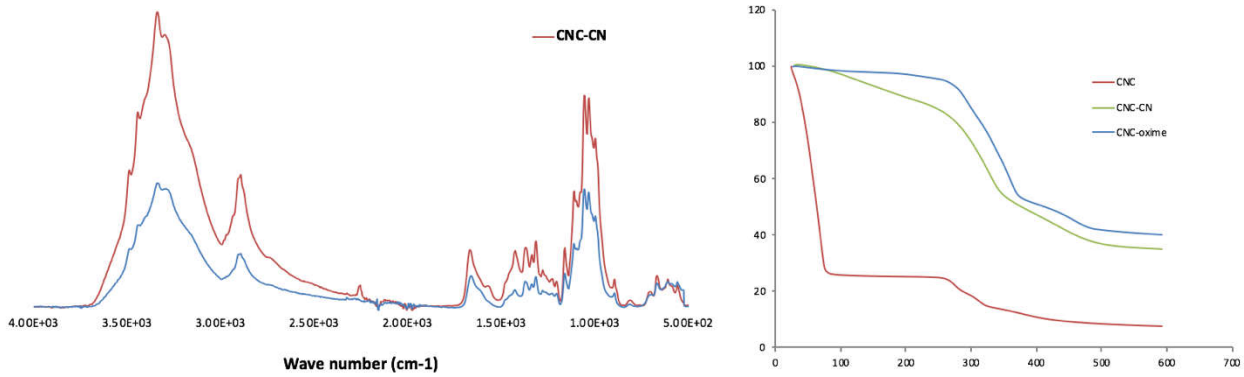

Figure 14. Infrared spectroscopy (left) and thermogravimetric analysis (right) demonstrating successful preparation of oxime-functionalized cellulose nano and microcrystals.

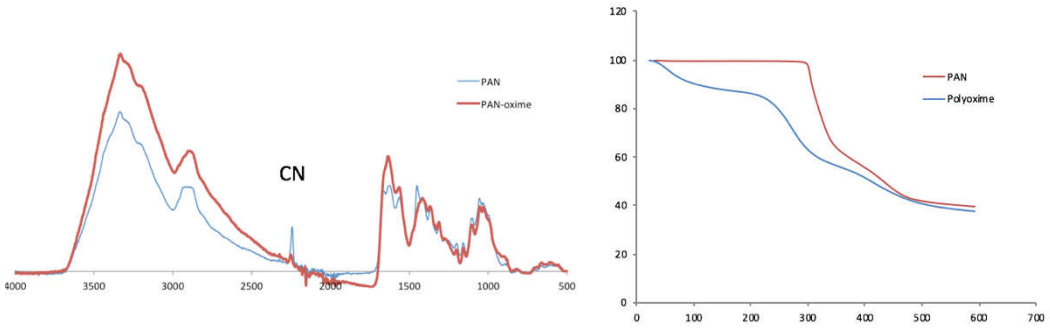

Figure 15. Infrared spectroscopy (left) and thermogravimetric analysis (right) demonstrating effective synthesis of poly(oxime) acrylonitrile polymer.

After the successful preparation of these three novel preparations, they were subjected to analysis for the removal of an organophosphorous pesticide from solvent (dichloromethane) and from

water. Unfortunately, none of the three appreciably changed the level of pesticide present in the water samples.

At this point, we abandoned our attempts to modify polymeric materials with oxime functional groups for the removal of pesticides. Instead, we shifted our focus toward the exploration of our poly(amine) grafted materials instead. The successful results of that study are the subject of the companion progress report for our current ACREC award.

Impacts and Significance: The technology described in this proposal has the potential to be very beneficial to the rendering industry in terms of providing a next-generation alternative to established methods for odor remediation. We envision that the Materials described herein might present several uses in an industrial setting. The particles could be employed as a rapid-use odor adsorbent in an emergency or spill situation. Further, the particles could, in principle, be incorporated into existing odor remediation equipment as an added means for odor elimination. The obvious long-term goal would be to develop an appropriate formulation of functionalized nanomaterials that would compete with or ideally supplant existing odor elimination measures.

We are moving ever closer toward the successful development of a commercially viable material for odor remediations.

Publications:

The following peer-reviewed publications arose from this work:

1. **Guerra, F. D.; Campbell, M. L.; Attia, M. F.; Whitehead, D. C.; Alexis, F. "Capture of aldehyde VOCs using a series of amine-functionalized cellulose nanocrystals" *ChemistrySelect*, **2018**, *3,* 5495-5501 (cover feature).
2. **Swasy, M. I.; Campbell, M. L.; Attia, M. F.; Guerra, F. D.; Smith, Jr., G. D.; Alexis, F.; Whitehead, D. C. "PEI-functionalized kaolinite clay for the capture of VOCs" **2018**, *Chemosphere*, **2018**, *213*, 19-24.
3. **Ateia, M.; Attia, M. F.; Maroli, A.; Tharayil, N.; Alexis, F.; Whitehead, D. C.; Karanfil, T. "Rapid Removal of Poly- and Perfluorinated Alkyl Substances by Poly(ethyenimine)-Functionalized Cellulose Microcrystals at Environmentally Relevant Conditions" *Environmental Science & Technology Letters* **2018**, *5*, 764-769.
4. **Swasy, M. I.; Attia, M. F.; Hawk, J. M.; Alexis, F.; Whitehead, D. C. "Amine-Functionalized Cellulose Nanocrystal Materials for Pesticide Remediation from Water" **2019**, *manuscript under review*.
5. Attia, M. F.; Swasy, M. I.; Alexis, F.; Whitehead, D. C. "Controllable design of naked and PEI-capped porous and nonporous PDLLA-PEG-COOH and PLGA microparticles exhibiting dual modalities for VOC adsorption" **2019**, *manuscript under review*.

Outside funding:

During this funding period, we were awarded a $10,000 supplemental grant from the South Carolina Research Authority.

Future Work: Leveraging current FPRF/ACREC support, we continue to aggressively pursue objectives geared toward scale-up and production cost reduction with the goal of commercializing the materials described herein. Our ultimate goal is to arrive at a commercially viable material that can be deployed for odor remediation in the rendering industry as well as other environmental applications.

Acknowledgments: Graduate students Maria Swasy, Chandima Narangoda, and Beau Brummel contributed to the work described in this report. Postdoctoral associates Dr. Mohamed Attia and Dr. Mohamed Ateia contributed to this report as well.